



Atomic Insights into the Melting Behavior of Metallic Nano-catalysts

Bahareh Mobedpour, Reza Roumina, Sina Rajabdoust*

School of Metallurgy and Materials Engineering, College of Engineering, University of Tehran, Tehran, Iran.

Received: 24 September 2017; Accepted: 27 October 2017

** Corresponding author email: roumina@ut.ac.ir*

ABSTRACT

In the present study, molecular dynamics simulations have been utilized to provide fundamental understanding of melting behavior of pure Pd and Pt nanoparticles with the size of 10 nm in diameter, both free and graphene-supported during continuous heating. The embedded atom method is employed to model the metal-metal interactions, whereas a Lennard-Jones potential is applied to describe the metal-carbon interactions. In addition, interactions between carbon atoms are defined by the adaptive intermolecular reactive bond order potential. Heating curves calculated between 298 K-2000 K are used to determine solid-liquid transitions. Based on simulation results, three approaches are used to investigate the thermal behavior of Pd and Pt nanoparticles. These include potential energy variation, the percentage of FCC atoms as a function of temperature and the mean square displacement method. Melting temperature of nanoparticles is found to decrease when the particles are supported by the graphene substrate. The decrease in melting temperature of particles is ascribed to the interaction of carbon atoms with nanoparticles. Structural changes during melting of nanoparticles are also detected through the common neighbor analysis and the mean square displacement method. The analyses of crystal structure shows that the supported nanoparticles melt from surface. In addition, a sharp increase in the mean square displacement of supported nanoparticles is observed after melting which is suggested to be responsible for the reduction of melting point of nanoparticles.

Keywords: *Molecular Dynamics; Platinum Nanoparticles; Palladium Nanoparticles; Graphene.*

How to cite this article:

Mobedpour B, Roumina R, Rajabdoust S. Atomic Insights into the Melting Behavior of Metallic Nano-catalysts. *J Ultrafine Grained Nanostruct Mater*, 2017; 50(2):81-89.

1. Introduction

Structural and thermal properties of nanoparticles are important because of their synthesis and applications. Due to the excellent reactivity and stability, large surface-to-volume ratios, quantum size and structure sensitivity effects in nano-scales, metal nanoparticles (NPs) play a significant role in many applications such as electronics, optics and catalysis [1-6]. In recent years, significant efforts have been carried out to improve catalytic activities by loading NPs onto

suitable supporting materials. The support can alter catalysts activity in different ways such as changing the structure and shape of the NPs, charge transfer to or from NPs and providing additional reaction sites [7]. In particular, carbon-supported Pt-based NPs are commonly used for hydrogen storage, oxygen reduction reaction, electrochemical sensing and fuel cell applications [8]. Fabrication routes for supported NPs can be categorized in three categories: physical (e.g. sonication, microwaves, UV), chemical (e.g. electrochemical, impregnation)

and physicochemical (i.e. sono-electrochemical) routes [9]. These routes are governed by thermodynamic principles which can be adjusted by synthetic parameters such as ligand type and ligand to metal ratios. These parameters affect the catalytic activity and selectivity by controlling the size of NPs [10]. Surfactants used for binding the surface of NPs as ligands, can control the structure and prevent coalescence of NPs by lowering the surface energy with modifying electronic structure of catalytic sites [11]. So, properties depending on surface energy including the melting temperature can change. In addition, it is found that many monometallic NPs such as Pd, Au, Pt and Ag efficiently dispersed on graphene supports exhibit impressive catalytic performance [12]. Graphene, a monolayer of carbon atoms densely packed into a two-dimensional honeycomb lattice, has recently received a great deal of attention due to its larger specific surface than graphite or carbon nanotubes [13], impressive mechanical properties [14], and unique electronic properties [15]. Therefore, graphene is a promising candidate for dispersing catalytically active metal NPs and it is important to determine thermal characteristics of graphene supported transition metal nanoclusters. Although there are few studies on graphene supported nanocatalysts, one main difficulty is the poor control of synthesis of NPs on the surface of graphene [12]. Furthermore, experimental techniques, i.e. diffraction and calorimetry, are not precise enough to study thermal behavior of catalysts at nanometer scale [16].

Molecular dynamics (MD) has been proven to be a useful technique for investigation of processes involving nanoparticle-support interface interactions at the atomic level. Huang and Balbuena [17] studied melting behavior of small Pt clusters on graphite for the first time and reported surface melting below the melting point. Later, Huang et al. [18] found that the Cu-Ni and Pt-Au bimetallic particles on graphite display slightly higher melting point than isolated nanoclusters of identical size and composition. Morrow and Striolo [19] studied Pt nanoparticles on carbon nanotube

and graphite. They explored that the diffusion coefficient of Pt nanoparticles on carbon nanotubes (CNTs) is one order of magnitude lower than the one on graphite. However, it is worth noting that Pt NPs trapped between CNTs possesses a lower surface area which is a serious drawback in catalyst application. Although extensive studies have been performed to design, synthesis, characterize and evaluate performance of NPs, there is still lacking a full atomic-level understanding of structural and thermal stabilities of NPs.

In the present work, MD simulations are conducted to study the thermal behavior of free and graphene supported pure Pt and Pd NPs. The entire previous studies considered the support to be static and hence relaxation of support was missed. Here, the particle-support interaction is considered to be more realistic by letting graphene substrate to move and relax in contact with the nanoparticle. The goal of the present study is to investigate the effect of carbon interactions on properties of supported metal NPs including the melting point, structure evolution and diffusion coefficient. The Pt-Pt and Pd-Pd interactions are modelled with embedded atom method (EAM) and the Pt-C and Pd-C interactions with a Lennard-Jones (LJ) potential. The interactions between carbon atoms are also defined by the adaptive intermolecular reactive bond order (AIREBO) potential. Finally, structural changes of NPs during a heating cycle are detected and the results are discussed.

2. Simulation Details

MD Calculations are performed using the Large-Scale Atomic/Molecular Massively Parallel Simulator (LAMMPS) [20], an open source program designed to simulate a large variety of different materials in atomic resolution. Initial models are constructed from pure Pt and Pd NPs on a graphene surface. The graphene sheet is considered to be 20×20 nm² made of 15936 atoms providing enough apparent area for allocating Pt and Pd nanoparticles with the same diameter of 10 nm. Pt and Pd NPs include 34881 and 35529 atoms respectively and are placed approximately

Table 1- LJ parameters of Pt-C and Pd-C interactions [23]

Material	$\epsilon(10^{-2} eV)$	$\sigma(\text{\AA})$
Pt-C	4.0922	2.936
Pd-C	3.3500	2.926

2 Å above a graphene support. Free standing Pt and Pd NPs with the same number of atoms mentioned above are also constructed.

The EAM method is used to model metal-metal interactions, as described by Foiles et al. [17]. The total potential energy in the EAM model is given by equation (1):

$$U = \sum_i F_i (\sum_{j \neq i} \rho_j(r_{ij})) + \frac{1}{2} \sum_i \sum_{i \neq j} \phi_{ij}(r_{ij}) \quad (\text{eq. 1})$$

where F_i is the energy required to embed atom i into the background electron density ρ_j , is the electron density due to atom j and $\phi_{ij}(r_{ij})$ is the repulsion between the cores of atoms i and j separated by a distance r_{ij} [21]. The force field parameters used to model Pt and Pd are included in the Pt_u3.eam and Pd_u3.eam potential files in the LAMMPS package, respectively.

To describe the carbon-carbon interactions in graphene, AIREBO potential is employed. This potential includes dispersion forces, intermolecular repulsion and torsional interactions. Equation (2) represents the formulation of AIREBO potential [22]:

$$E = \frac{1}{2} \sum_i \sum_{j \neq i} [E_{ij}^{REBO} + E_{ij}^{LJ} + \sum_{k \neq i, j} \sum_{l \neq i, j, k} E_{kijl}^{TORSION}] \quad (\text{eq. 2})$$

The metal-carbon interaction is modeled via a 12-6 LJ potential [23]. Equation (3) represents the formulation of LJ potential:

$$E_i = \sum_{j \neq i} 4\epsilon [(\frac{\sigma}{r_{ij}})^{12} - (\frac{\sigma}{r_{ij}})^6] \quad (\text{eq. 3})$$

where ϵ is the depth of potential well, σ is the distance at which the potential is zero, and r_{ij} the distance between atoms i and j [24]. The LJ parameters are obtained from [23], listed in Table 1.

The time integration of the equation of the motion is performed utilizing the Verlet Algorithm [21] with a time step of 3 fs. These conditions are designed to generate positions and velocities sampled from canonical (NVT) ensemble and the temperature is controlled by the Nosé-Hoover thermostat method. First, the system is relaxed for 10^6 time steps, for a total of 3 ns at 298 K, then heated up from 298 K to 2000 K in 3 μs. Finally, the relaxation process is repeated for 3 ns. Periodic boundary conditions are used to avoid problems with boundary effects caused by the finite size of graphene. Same parameters are used for heating both free standing and supported NPs.

3. Results and Discussion

3.1. Potential Energy

Melting behavior of NPs is determined by using three different approaches. First, the potential energy variation of free and supported NPs is plotted versus temperature as shown in Figures 1 (a) and 2 (a). The potential energy of supported ones includes both the metal-substrate interactions as well as the metal-metal interactions. These figures clearly illustrate a jump in the so called potential energy curve corresponding to the melting transition. The variation of potential energy with increasing temperature is clearly presented by increasing the number of red atoms with higher potential energy at the particle surface (Figure 1 (b) and Figure 2 (b)).

Thermodynamic properties of NPs strongly depends on the size which is mainly associated with the fraction of surface atoms. The surface to volume ratio obeys the invert scaling law and atoms on the surface have a lower coordination number than inner ones due to the presence of breaking bonds. Therefore, by reducing the size of a nano-particle the energy of system increases [26]. Consequently, the surface-dependent properties such as melting point and crystal structure may change. The melting temperature of NPs is normally below the bulk melting point temperature and decreases with cluster size [27] but our simulations investigate a specific size of NPs with 10 nm in diameter. One may expect that even by further reducing the size of a nano-particle from 10 nm to much smaller sizes such as 1 nm, the melting point temperature decreases significantly. According to Figures 1(a) and 2(a), the graphene supported Pt and Pd NPs start to melt at 1530 K and 1430 K, respectively while the free standing counterparts melt at 1650 K and 1570 K, respectively. These results are consistent with the fact that the melting temperature of free standing and supported NPs is lower than the melting point of bulk ones [27]. It is also found that the melting temperature of supported NPs is lower than the one for free NPs. According to Figures 1(a) and 2(a), in the solid-liquid transition region at a given temperature, the potential energy curve for supported NPs is above the one for free standing NPs. The increase in potential energy accelerates atomic vibration and therefore melting occurs at lower temperatures. This increase in potential energy can be related to the metal-carbon interactions which are confirmed by capping NPs on the graphene support near the

melting point as illustrated in Figures 1(b) and 2(b). In addition, Figures 1(a) and 2 (a) show the

deviations from linearity in the potential energy curves of supported ones which indicate the

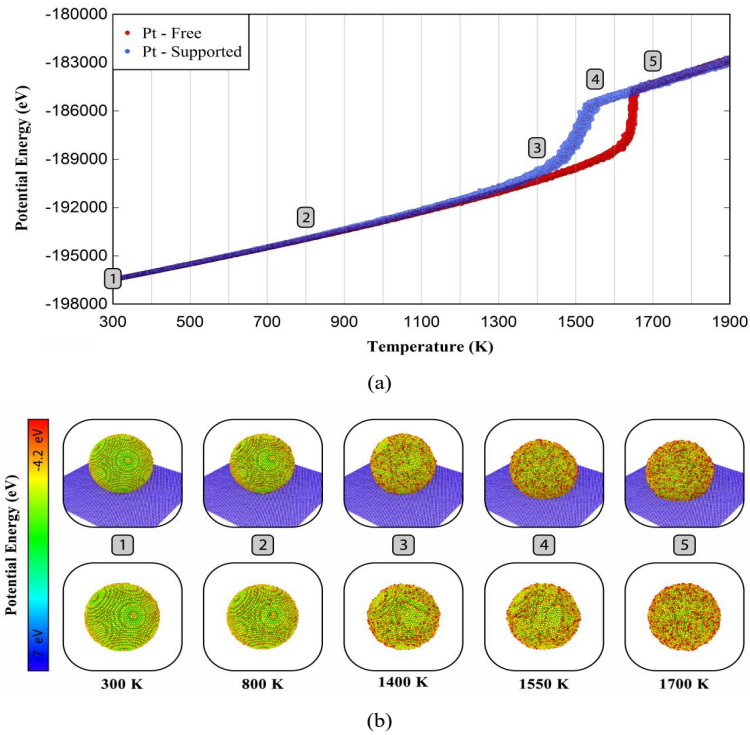


Fig. 1- (a) Potential energy versus temperature and (b) the corresponding snapshots for free and supported Pt NPs.

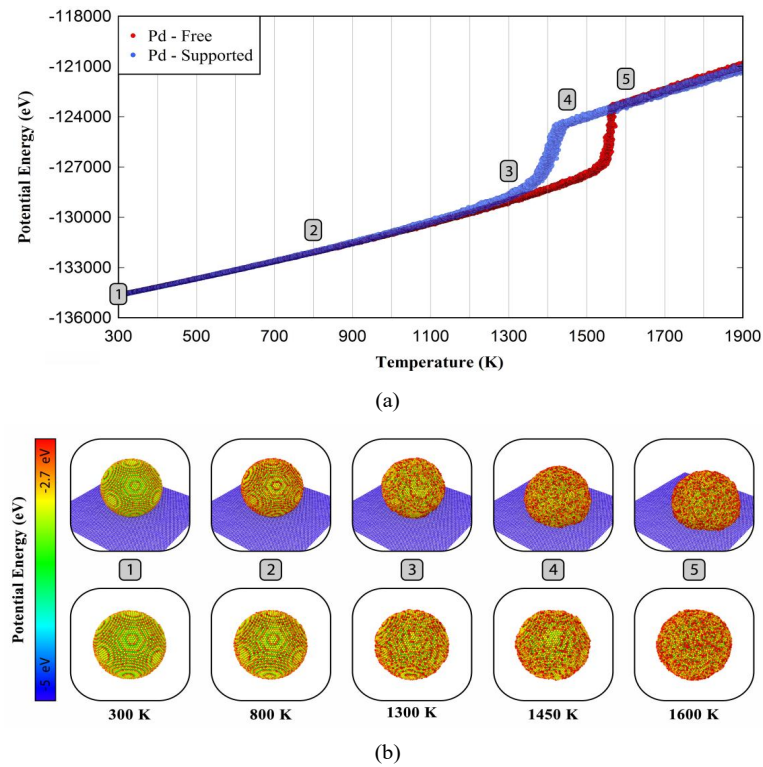


Fig. 2- (a) Potential energy versus temperature and (b) the corresponding snapshots for free and supported Pd NPs.

tendency of the supported NPs to surface melting but free ones melt homogeneously. This difference of melting behavior is shown by the common neighbor analysis (CNA) in the next section.

In order to show the difference of melting point for free and supported NPs, the potential energies of NPs are divided by the number of their atoms so the variations of energy are reported as normalized values in Figure 3. This Figure illustrates that supported NPs melt at lower temperatures than free ones. Furthermore, both free and supported Pd and Pt NPs melt at lower temperatures than bulk Pt and Pd.

Although we simulate NPs having the same size in both free and supported conditions, the size effect can impact metal-carbon interactions. The NPs size effect on the interaction with the support is the combination of dispersion interactions and adsorption energy. The nanoparticle size affects the number of atoms at the interface of metal-graphene. The dispersion interactions increase with the size of NPs but the adsorption energy of metal-carbon decreases. For large NPs such as our system, it is expected that the dispersion interactions are dominant [28]. Therefore, the size effect change the metal-carbon interactions which affects the potential energy of the system. The free and supported NPs display different melting points in our simulations due to the metal-

carbon interaction. In addition, the influence of temperature should not be ignored on metal-carbon interactions. The temperature-dependent potential energy plots in Figure 1 interpret that by increasing temperature, atomic vibrations rise up. The sphere shape of NPs change to a cap on the substrate thereby increasing the contact area between NPs and the graphene support. Finally, by increasing temperature metal-carbon interactions as well as the potential energy of supported NPs increase which could be the cause of the melting point reduction of supported NPs.

3.2. Common Neighbor Analysis (CNA)

The second approach for investigating melting behavior is monitoring the percentage of FCC atoms as a function of temperature. Recently, CNA method has been proven to be a useful tool for defining melting temperature as it provides the possibility of identifying the local crystal structure. This method determines crystal structure of each cluster based on a nearest-neighbor graph that encodes the bond connectivity among neighbors of a given central particle [29]. The evolution of crystal structure for both free and supported NPs is shown in Figures 4 and 5. The crystal structure of crystalline materials disappears completely at the melting point. Figures 4 and 5 demonstrate that the degree of crystallinity for both Pt and Pd NPs decreases

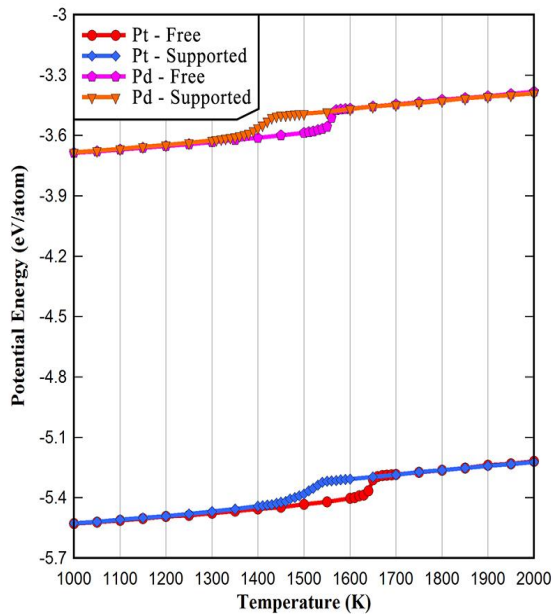


Fig. 3- Variations of normalized potential energies for both free and supported Pt and Pd NPs.

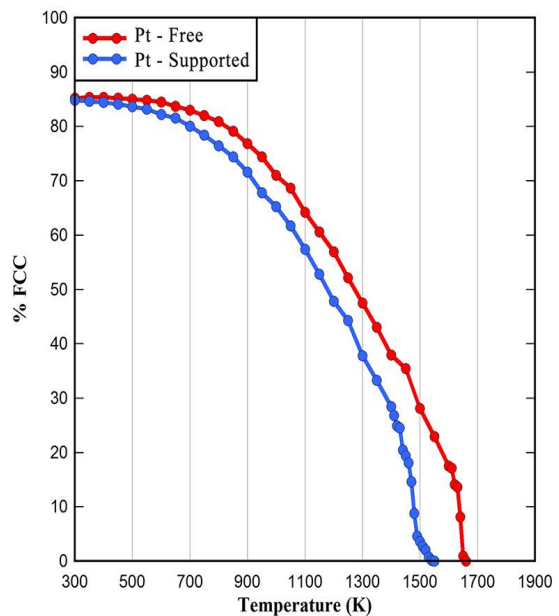


Fig. 4- Percentage variation of FCC atoms by increasing temperature in both free and supported Pt NPs.

sharply near the melting point and their crystal structures become disordered completely at their melting point. Based on simulation results given in Figures 4 and 5, melting point temperatures for supported and free Pt NPs are 1530 K and 1650 K, respectively. Also melting point temperatures for supported and free Pd NPs are found to be 1430 K and 1570 K, respectively. Simulation results presented in this section are in agreement with the ones presented in Figures 1 and 2.

It is known that large reduction in surface energy is responsible for embedding particles at interfaces [30]. This is commonly explained by

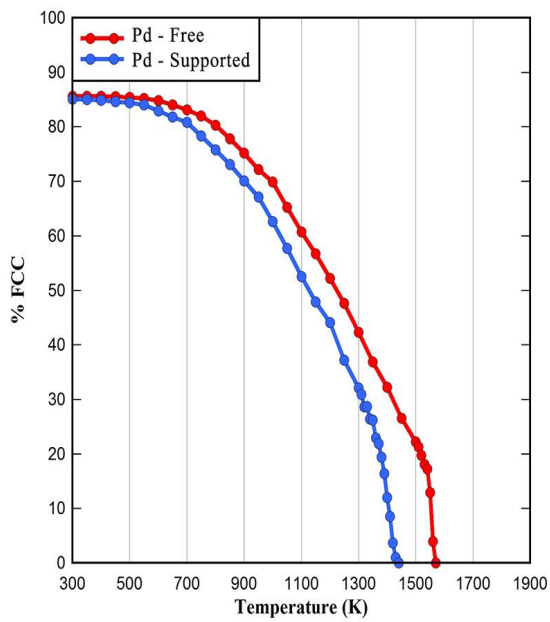


Fig. 5- Percentage variation of FCC atoms by increasing temperature in both free and supported Pd NPs.

the reduction of particle interface in one phase and developing its interface with a second phase. There are evidences of particle sinking at elevated temperatures [31, 32]. As mentioned in the previous section, supported and free metallic particles show different melting behavior due to metal-carbon interactions. Different melting behavior for supported and free standing NPs as a result of metal-carbon interactions is confirmed in Figures 6 and 7 illustrating cross sections of NPs during heating. The metal-carbon interaction causes particle sinking on graphene in order to reduce the surface energy. Therefore, distortion appears and the crystal structure disappears at the interface. The disordered structure of the interface could be the main cause of surface melting in supported NPs.

3.3. Mean Square Displacement (MSD)

Calculation the Mean Square Displacement (MSD) is the third approach for studying melting behavior of NPs. In addition to the structural evolution of NPs during continuous heating, the diffusion behavior of atoms in NPs is also an important issue which needs to be addressed due to its technological aspects for processing catalysts. The thermally driven diffusion is generally evaluated by the diffusion coefficient D , which can be calculated from the mean-square displacement (MSD) [33]. The self-diffusion coefficient D_i can be obtained from the three-dimensional mean square displacement [23]:

$$D = \frac{1}{6\Delta t} [r_i(t+k) - r_i(k)]^2 \quad (\text{eq. 4})$$

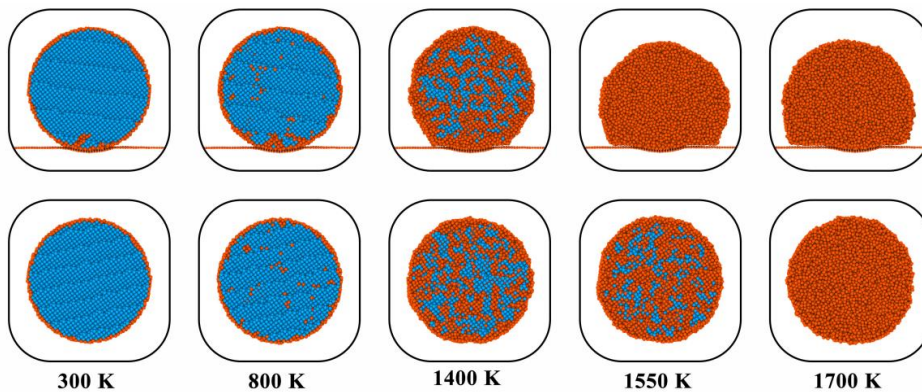


Fig. 6- Snapshots of changing crystal structure from crystalline to amorphous (disordered) by distortion at the interface of graphene and increasing temperature in Pt NPs. The upper and lower rows represent supported and free standing NPs, respectively. (blue and orange colors show FCC and amorphous structures, respectively).

where $r_i(t)$ represents the vector position of the i th atom at time t with averages taken over k time steps. In this manner, the relative change of diffusivity of atoms at different temperatures is more evident from computing the MSD parameter. The calculated MSDs for all NPs are given in Figures 8 and 9. A sharp increase in MSD is observed at the melting point of NPs and this increase is more significant for NPs supported with graphene. In other words, the supported NPs have higher self-diffusion coefficients than the free ones. Supported NPs absorb graphene substrate to reduce the

surface energy. By increasing temperature, the surface to volume ratios rises and NPs form spherical cap. On the other hand, the distortion at the interface of graphene with the particle makes the crystal structure disordered. Large surface to volume ratio of the particle on graphene and the disordered structure at the interface lead to higher MSDs for supported NPs.

Figure 10 depicts that the MSD ratio of Pd NPs near the melting point is about 6 times higher than Pt ones. This difference in diffusivity is mainly associated with the difference of surface energy

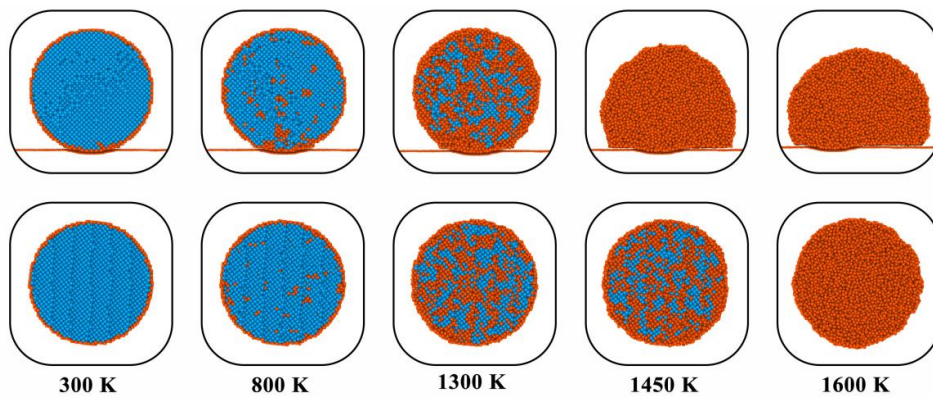


Fig. 7- Snapshots of changing crystal structure from crystalline to amorphous (disordered) by distortion at the interface of graphene and increasing temperature in Pd NPs. The upper and lower rows represent supported and free standing NPs, respectively. (blue and orange colors show FCC and amorphous structures, respectively).

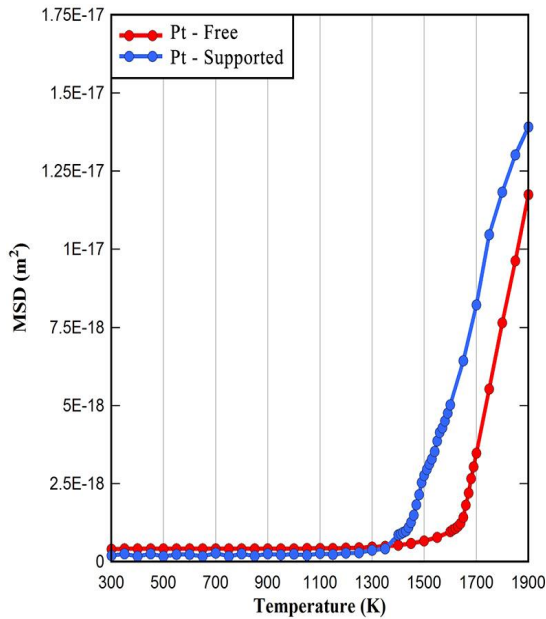


Fig. 8- Mean-square displacement versus temperature for Pt NPs.

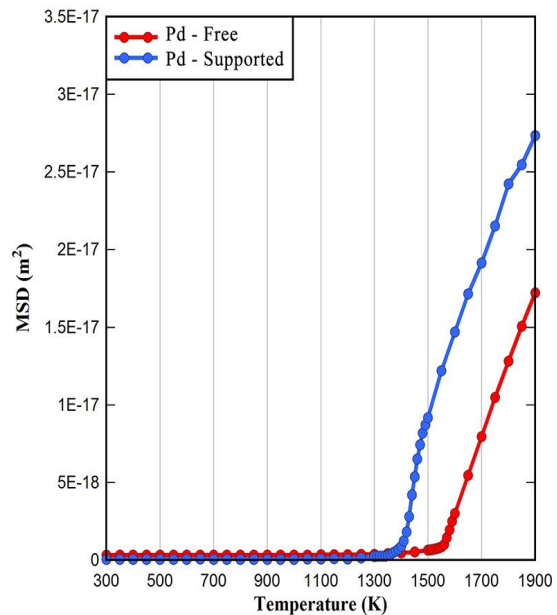


Fig. 9- Mean-square displacement versus temperature for Pd NPs.

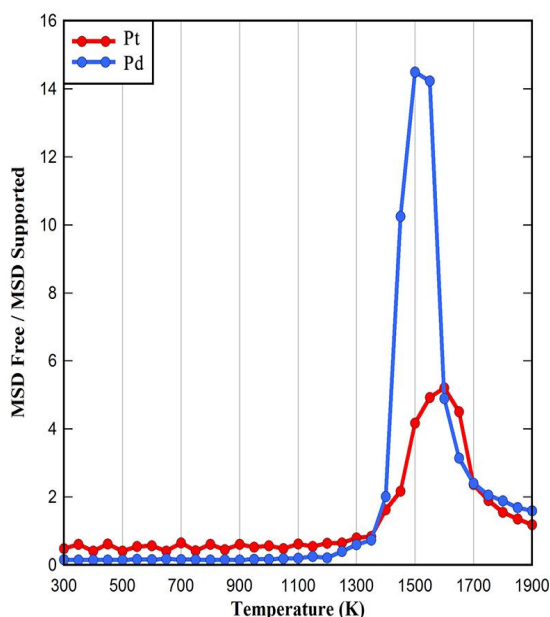


Fig. 10- Mean-square displacement ratio versus temperature for free and supported Pt and Pd NPs.

of Pd and Pt atoms as the surface energy of Pd is smaller than the surface energy for Pt [34].

4. Conclusions

In summary, atomistic simulations have been employed to examine the melting behavior of metallic NPs, free standing and supported with graphene, during continuous heating. The melting behavior of free particles is compared with the ones for supported particles on a graphene substrate. The melting point for supported NPs is about 130 K lower than the melting point of free ones. This can be attributed to the increased metal-substrate interaction resulting from capping of NPs on the graphene support by increasing temperature. We observe that the melting behavior of supported and free NPs is different due to the disordered structure at the metal-substrate interface. Moreover, it is found that self-diffusion coefficients for NPs on the graphene support are higher than the ones for free NPs. The larger self-diffusion coefficients stem from larger surface to volume ratio of particles on the graphene substrate and the disordered structure at the interface. These results suggest that the thermal properties of NPs can be tailored through adjusting the material for the substrate. The implications of these conclusions can be extended to other NPs. Due to the potential utility of NPs in catalysis, the present study is expected to be important not only for exploring the catalytic

activity of NPs but also for further design of multi-metallic nanostructures. Finally, the outcome of the present study can be extended to bi-metallic NPs for future investigations.

References:

- Garcia MA. Surface plasmons in metallic nanoparticles: fundamentals and applications. *Journal of Physics D: Applied Physics*. 2011;44(28):283001.
- Warrier P, Teja A. Effect of particle size on the thermal conductivity of nanofluids containing metallic nanoparticles. *Nanoscale Research Letters*. 2011;6(1):247.
- Leppard G., Mavrocordatos D., Perret D. Electron-optical characterization of nano- and microparticles in raw and treated waters: an overview. *Journal of Water Science and Technology*. 2004;50(12):1-8.
- Govorov AO, Richardson HH. Generating heat with metal nanoparticles. *Nano Today*. 2007;2(1):30-8.
- Lattuada M, Hatton TA. Synthesis, properties and applications of Janus nanoparticles. *Nano Today*. 2011;6(3):286-308.
- Thompson DT. Using gold nanoparticles for catalysis. *Nano Today*. 2007;2(4):40-3.
- Cuenya BR. Synthesis and catalytic properties of metal nanoparticles: Size, shape, support, composition, and oxidation state effects. *Thin Solid Films*. 2010;518(12):3127-50.
- Joo SH, Park JY, Tsung C-K, Yamada Y, Yang P, Somorjai GA. Thermally stable Pt/mesoporous silica core-shell nanocatalysts for high-temperature reactions. *Nature Materials*. 2008;8(2):126-31.
- Campelo JM, Luna D, Luque R, Marinas JM, Romero AA. Sustainable Preparation of Supported Metal Nanoparticles and Their Applications in Catalysis. *ChemSusChem*. 2009;2(1):18-45.
- Mozaffari S, Li W, Thompson C, Ivanov S, Seifert S, Lee B, et al. Colloidal nanoparticle size control: experimental and kinetic modeling investigation of the ligand-metal binding role in controlling the nucleation and growth kinetics. *Nanoscale*. 2017;9(36):13772-85.
- Jin L, Liu B, Duay S, He J. Engineering Surface Ligands of Noble Metal Nanocatalysts in Tuning the Product Selectivity. *Catalysts*. 2017;7(2):44.
- Chen H, Li Y, Zhang F, Zhang G, Fan X. Graphene supported Au-Pd bimetallic nanoparticles with core-shell structures and superior peroxidase-like activities. *Journal of Materials Chemistry*. 2011;21(44):17658.
- Stoller MD, Park S, Zhu Y, An J, Ruoff RS. Graphene-Based Ultracapacitors. *Nano Letters*. 2008;8(10):3498-502.
- Lee C, Wei X, Kysar JW, Hone J. Measurement of the Elastic Properties and Intrinsic Strength of Monolayer Graphene. *Science*. 2008;321(5887):385-8.
- Castro Neto AH, Guinea F, Peres NMR, Novoselov KS, Geim AK. The electronic properties of graphene. *Reviews of Modern Physics*. 2009;81(1):109-62.
- Baletto F, Ferrando R. Structural properties of nanoclusters: Energetic, thermodynamic, and kinetic effects. *Reviews of Modern Physics*. 2005;77(1):371-423.
- Ping S-P, Balbuena PB. Platinum nanoclusters on graphite substrates: a molecular dynamics study. *Molecular Physics*. 2002;100(13):2165-74.
- Huang S-P, Mainardi DS, Balbuena PB. Structure and dynamics of graphite-supported bimetallic nanoclusters. *Surface Science*. 2003;545(3):163-79.
- Morrow BH, Striolo A. Morphology and Diffusion Mechanism of Platinum Nanoparticles on Carbon Nanotube Bundles†. *The*

- Journal of Physical Chemistry C. 2007;111(48):17905-13.
20. Plimpton S. Fast Parallel Algorithms for Short-Range Molecular Dynamics. *Journal of Computational Physics*. 1995;117(1):1-19.
 21. Foiles SM, Baskes MI, Daw MS. Embedded-atom-method functions for the fcc metals Cu, Ag, Au, Ni, Pd, Pt, and their alloys. *Physical Review B*. 1986;33(12):7983-91.
 22. Stuart SJ, Tutein AB, Harrison JA. A reactive potential for hydrocarbons with intermolecular interactions. *The Journal of Chemical Physics*. 2000;112(14):6472-86.
 23. Sankaranarayanan SKRS, Bhethanabotla VR, Joseph B. Molecular dynamics simulations of the structural and dynamic properties of graphite-supported bimetallic transition metal clusters. *Physical Review B*. 2005;72(19).
 24. Sato S, Chen D-R, Pui DYH. Molecular Dynamics Study of Nanoparticle Collision with a Surface – Implication to Nanoparticle Filtration. *Aerosol and Air Quality Research*. 2007;7(3):278-303.
 25. Verlet L. Computer “Experiments” on Classical Fluids. I. Thermodynamical Properties of Lennard-Jones Molecules. *Physical Review*. 1967;159(1):98-103.
 26. Roduner E. Size matters: why nanomaterials are different. *Chemical Society Reviews*. 2006;35(7):583.
 27. Gupta SK, Talati M, Jha PK. Shape and Size Dependent Melting Point Temperature of Nanoparticles. *Materials Science Forum*. 2008;570:132-7.
 28. Verga LG, Aarons J, Sarwar M, Thompson D, Russell AE, Skylaris CK. Effect of graphene support on large Pt nanoparticles. *Phys Chem Chem Phys*. 2016;18(48):32713-22.
 29. Honeycutt JD, Andersen HC. Molecular dynamics study of melting and freezing of small Lennard-Jones clusters. *The Journal of Physical Chemistry*. 1987;91(19):4950-63.
 30. Kaz DM, McGorty R, Mani M, Brenner MP, Manoharan VN. Physical ageing of the contact line on colloidal particles at liquid interfaces. *Nature Materials*. 2011;11(2):138-42.
 31. Yang XF, Xi XM. Formation of pits on ceramic surfaces coated with gold. *Journal of Materials Research*. 1994;9(10):2484-6.
 32. Karakouz T, Maoz BM, Lando G, Vaskevich A, Rubinstein I. Stabilization of Gold Nanoparticle Films on Glass by Thermal Embedding. *ACS Applied Materials & Interfaces*. 2011;3(4):978-87.
 33. Huang R, Wen Y-H, Zhu Z-Z, Sun S-G. Two-Stage Melting in Core-Shell Nanoparticles: An Atomic-Scale Perspective. *The Journal of Physical Chemistry C*. 2012;116(21):11837-41.
 34. Vitos L, Ruban AV, Skriver HL, Kollár J. The surface energy of metals. *Surface Science*. 1998;411(1-2):186-202.